Catena 195 (2020) 104896

Contents lists available at ScienceDirect

Catena

journal homepage: www.elsevier.com/locate/catena

Characteristics of small anthropogenic landforms resulting from historical charcoal production in western Connecticut, USA

Alexander Bonhage[a,*], Florian Hirsch[a], Thomas Raab[a], Anna Schneider[a], Alexandra Raab[b], Will Ouimet[c]

[a] Brandenburg University of Technology Cottbus-Senftenberg, Chair of Geopedology and Landscape Development, Germany
[b] Brandenburg University of Technology Cottbus-Senftenberg, Chair of Evironmental Economics, Germany
[c] University of Connecticut, Department of Geography and Center for Integrative Geosciences, USA

ARTICLE INFO

Keywords:
Pedostratigraphy
Historical charcoal production
Relict charcoal hearth
Bulk density
Geoarchaeology
Technosol

ABSTRACT

Relict charcoal hearths (RCHs) are anthropogenic geomorphic features with an average diameter of 12 m found in many forests of Central Europe and in the eastern USA wherever pre-coal iron production took place or other industries demanded the production of charcoal. To expand the knowledge about their geoarchaeological significance and their legacy effect on soil properties and forest ecosystems, we propose a method for a generalized description of soil stratigraphy on RCHs. We studied 154 soil profiles at 52 RCH sites alongside two 1 km transects in Litchfield County, Connecticut, USA. The sites can be classified based on the slope inclination, with sites on $< 4^\circ$ mostly having a single-layered stratigraphy and an elevated circular shape, while sites on slopes $> 4^\circ$ mostly are built as levelled and multilayered platforms. The latter have two or more charcoal rich technogenic Auh-layers separated by intermediate Auh-layers mostly consisting of mineral substrate. Based on average layer thicknesses and their dependence on the sites slope inclinations, we propose a model with two idealized RCH shapes with slope controlled properties that allow for an easy computation of site diameters and elemental stocks. With ongoing advances in remote sensing of RCH sites, our proposed model can help to further understand the effects of historic land use on a landscape scale.

1. Introduction

Relict charcoal hearths (RCH) are anthropogenic geomorphic features with an average diameter of 12 m found mainly in forests of historical mining areas and are therefore part of the sociocultural fingerprint on many landscapes (Tarolli et al., 2019). They mark the position of former charcoal production sites that supplied local industries before the use of coal (Ludemann, 2010). RCHs are detectable in the field and by remote sensing on LiDAR-derived digital elevation models (DEMs) (Schneider et al., 2020a,b, Rutkiewicz et al., 2019, Johnson et al., 2015). They are visible as levelled, near circular platforms built into slopes or as circular elevations on flat terrain (Hirsch et al., 2018a). They typically consist of at least one layer of technogenic substrate (Auh-horizon, IUSS Working Group WRB, 2014) that can be multiple decimeters thick and is heavily enriched in charcoal. Soils in forests that are influenced by historical charcoal burning display documented changes in vegetation (Buras et al., 2020, Mastrolonardo et al., 2019, Carrari et al., 2018, Mikan and Abrams, 1995) and faunal growth (Gießelmann et al., 2019). However, the specific drivers of these changes are unknown so far. Beside a clear increase in the soil organic matter (SOM) content (Bonhage et al., 2020, Mastrolonardo et al., 2018, Hardy et al., 2016, Borchard et al., 2014), some studies document an increase in soil nutrient stocks (Buras et al., 2020, Borchard et al., 2014) and a positive effect on the cation exchange capacity (CEC) (Mastrolonardo et al., 2019, Hardy et al., 2017, Mikan and Abrams, 1995). However, these impacts are not confirmed for other study areas (Hirsch et al., 2018b). Multiple changes in soil physical properties like bulk density, water infiltration patterns and thermal conductivity compared to reference forest soils have been found in recent studies (Schneider et al., 2020a,b, 2019, 2018a). Furthermore, RCH sites are a subject of studies in anthracology (Dupin et al., 2017, Knapp et al., 2015), palaeothermometry (Dupin et al., 2019) and the reconstruction of past fuel wood exploitation of forests (e.g. Tolksdorf et al., 2015, Ludemann, 2010). They often are of interest in the realm of DEM-based automated feature extraction using deep learning techniques (e.g. Verschoof-van der Vaart and Lambers, 2019). Overall, the list of current literature is showing a growing multidisciplinary interest in the study of historic charcoal production sites to understand the long-term influence

* Corresponding author at: Brandenburg University Technology Cottbus-Senftenberg, Siemens-Halske-Ring 8, 03046 Cottbus, Germany.
E-mail address: Alexander.Bonhage@b-tu.de (A. Bonhage).

https://doi.org/10.1016/j.catena.2020.104896
Received 11 May 2020; Received in revised form 25 August 2020; Accepted 31 August 2020
Available online 18 September 2020
0341-8162/

of charcoal addition to forest soils and forest ecosystems.

In their 2017 study, Raab et al. analyzed stratigraphical properties of 18 RCH sites on multiple locations in Litchfield County, Connecticut, USA, and concluded that local forest soils are heavily influenced by historical charcoal burning and the building technique of RCHs is comparable to sites in Europe. However, the small number of sites described in the Raab et al. study did not allow for generalizable soil sequences on RCHs with differing specifications such as size and topographic position (local slope). In this study, we analyze the variation of RCH soil stratigraphy and layer geometry on two separate, coherent topographic transects with regularly spaced RCHs that cover a wide range of topographical positions in terms of their slope inclination. We examine the pedostratigraphy of 153 soil profiles at 52 RCHs and their correlation with the topographical position to develop a RCH classification based on slope inclination. We also analyze variation of bulk density as a proxy for physical soil properties. We want to create a model consisting of generalized shapes of RCHs and soil stratigraphy that could potentially help in the upscaling of site specific physical and chemical soil properties to a regional or landscape scale. This would allow for fully assessing the legacy effects of historical charcoal production on today's soil landscapes and forest ecosystems.

2. Study area

The study area is located approximately 7 km north-east of the town West Cornwall in Litchfield County, Connecticut, USA. The area is part of the Appalachian Highlands with glacial sediments dominated by tills from the Wisconsin glaciation (Stone et al., 2005). The main morphological units are till-mantled hillslopes with narrow floodplains from the Housatonic River (Stone et al., 2005, Raab et al., 2017). The vegetation consists of maple, oak, birch and aspen forest (Raab et al., 2017). The climate is temperate with an annual mean temperature of 8.2 °C and a mean annual precipitation of 1164 mm. Soils are classified as Typic Dystrudepts (US Soil Taxonomy) or Cambisols (IUSS Working Group WRB, 2014) developed on fine sand dominated sandy loam, with an acidity that ranges from very strong to strongly acidic (pH 3.3–4.2, $CaCl_2$) (Hirsch et al., 2018a, Raab et al., 2017). Soils on RCHs are Anthropic Udorthents (US Soil Taxonomy) or Spolic Technosols (Humic) (IUSS Working Group WRB, 2014) (Hirsch et al., 2018a). RCHs in the area often have a multi-layered stratigraphy with charcoal rich Auh-layers and intermediate layers consisting of relocated mineral substrate (hereinafter referred to as intermediate Auh-layers). These intermediate layers are most likely not the result of in situ pedogenic processes or of erosive slopewash, but rather have their origin in the purposeful relocation of adjacent mineral substrate to enlarge or to renew the platform for further hearth operations (Raab et al., 2017, Hirsch et al., 2018a).

Besides RCHs there are further signs of historic anthropogenic activity in the study area, such as building foundations, old roads and stone walls, the latter are related to agricultural land use activities beginning in the early 18th century (Johnson and Ouimet, 2014). Although no direct dating's of RCHs are available, they can be indirectly dated by proxy of the blast furnaces operating in the area, which would mean they were most likely built between 1750 and 1850 (Raab et al., 2017). During this time period the area was deforested, as shown by historical documents (Raab et al., 2017). There is no evidence for other deforestations after this time period.

3. Field measurements and laboratory analysis

We surveyed RCH sites adjacent to two topographic transects, approximately 2 km apart, on a total area of 0.7 km^2 (Fig. 1). The transects were chosen in areas with the same surface geology and vegetation and to cover the characteristic topographic units with slopes of varying inclination and relatively flat areas in plateau or floodplain positions. Each transect consists of surficial geology characterized as thin glacial till mapped at 1:125,000 scale. RCH sites to be surveyed were chosen on a LiDAR DEM prior to field work based on their proximity to the idealized lines of the two transects. In total, 52 RCH sites were measured for their stratigraphy, diameter and surrounding slope inclination. To account for possible small scale variations in soil layer thickness, soil profiles where described for three 1 × 1 m soil pits for each RCH site. The location of the soil pits was determined according to the survey pattern shown in Fig. 2 to enable the reconstruction of the complete RCHs stratigraphy orthogonally to the slope. Position 1 is located at the upslope end, position 2 in the middle and position 3 at the downslope end of each RCH site. In case of a very flat relief at a site, we used the general slope of the landscape to determine position 1 and 2. One reference forest soil profile was dug for each site in a downslope position and a distance within 10–15 m from the site (Position 4). Soil profiles were usually dug to a depth that reaches the C-horizon, except when this was impossible because of large amount of rocks. The Auh-layers were completely measured in any case. The diameter of each site was measured orthogonally and parallel to the slope. The transects are named after nearby street designations. In the eastern end of the study area, the transect “Hollenbeck”, has a length of 920 m and an altitude ranging from 381 m to 440 m a.s.l. The western transect, “Wickwire”, has a length of 1100 m and an altitude ranging from 316 m to 375 m a.s.l. We analyzed 26 RCH sites adjacent to each transect (Fig. 1). The site specific slope inclination for each RCH was measured trigonometrically using adjacent elevations from a 1 m LiDAR DEM (horizontal accuracy ± 1 m, vertical accuracy 0.138–0.170 m, CTECO, http://www.cteco.uconn.edu/) taken parallel to the upslope-downslope orientation of the soil pits.

All soil profiles were sampled volumetrically in 5 cm vertical spacings with 250 ml steel cylinders and additionally in 10 cm steps as bulk samples. The bulk density was calculated based on 40 °C dry weight of the volumetric samples. Grain-size distribution of representative soil profiles was analyzed by wet sieving and fractionation according to the Soil Survey Investigation Report No. 42 method 3A1a1a. Soil pH was measured in 0.01 M $CaCl_2$. Descriptive and comparative statistics were done using ArcGIS 10.4.1 (ESRI) and SPSS 25 (IBM). For descriptive statistics of soil horizon thicknesses and bulk densities, any observation 1.5 times the interquartile range from Q1 and Q3 respectively, was treated as an outlier and was not included in further calculations. Significant differences between samples were determined using Mann-Whitney-U tests. LiDAR derived DEM visualizations were created using the Relief Visualization toolbox 2.2.1 and the Visualization for Archaeological Topography (VAT) method (Kokalj and Somrak, 2019).

4. Results

4.1. RCH classification and size

There are two typical architectural types of RCHs in the study area that are previously described for locations in Central Europe and the Eastern United States: RCHs on slopes and RCHs on flatland. RCHs on slopes consist of a levelled, slightly oval platform built into the slope, often framed by a stone wall at the downslope end. At most sites, they feature multiple charcoal rich Auh-layers with an increasing thickness towards the downslope end of the platform. RCHs on flatland are round, circular elevations of multiple decimeters, usually consisting of one charcoal rich Auh-layer whose thickness does not vary substantially for different positions on the site. For a detailed description of the genesis and historical background of these two typical architectural types we refer to Hirsch et al. (2020), Hirsch et al. (2018a) and Raab et al. (2017). Most common in our study area are RCH platforms on slopes (n = 34) and circular RCHs surrounded by a ditch on flatter terrain (n = 15). However, the ditches of the circular RCHs are not as pronounced and filled with charcoal as reported in other studies, therefore subsequent analysis will omit them from generalizations. Wickwire has 7 flat- and 19 platform RCHs on slopes while Hollenbeck has 8 flat- and

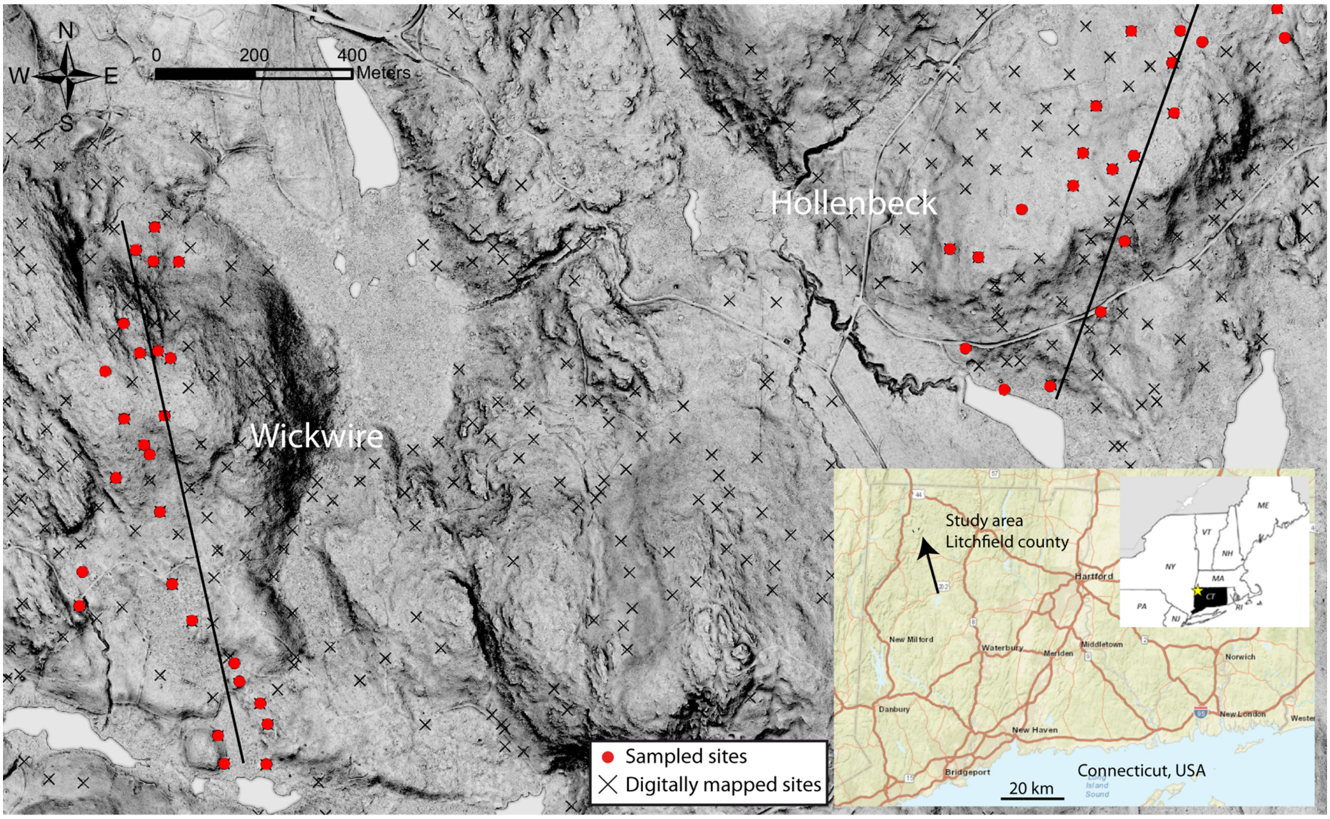

Fig. 1. Location of the transects "Wickwire" and "Hollenbeck" depicted on a 1 m LiDAR DEM. Red signatures mark the position of analyzed RCHs. Site coordinates are provided in Appendix F. LiDAR data courtesy of the Connecticut Department of Energy and Environmental Protection (CTECO, http://www.cteco.uconn.edu/). (For interpretation of the references to color in this figure legend, the reader is referred to the web version of this article.)

15 slope RCHs (Tables 1 and 2).

Soil physical and chemical properties of a representative site (Appendix A) are in accordance with results from former studies in this area. The soils are predominantly sandy loams dominated by coarse–-fine sand (Appendix E). Fig. 2 illustrates characteristic stratigraphy of both RCH types, showing the typical visual difference between both types, i.e. the occurrence or absence of charcoal rich- and intermediate Auh strata, mostly in position 2 and 3 of a site. However, this visual difference is not always present. We analyzed one multilayered RCH on flat terrain with an intermediate Auh-layer and eleven RCHs on steeper slopes with only one discernible Auh-layer. A definitive decision for classification was consequently based on a clear increase in summarized Auh- and intermediate Auh-layer thickness between the first and the third profile position of a site. This ratio is given as percentage value (ΔT) in Tables 1 and 2, with positive values showing an increase in Auh-layer thickness in the downslope direction, and negative values showing a decrease.

We set the threshold value for classifying sites to be ΔT $<$ or $>$ 50% (Fig. 3), as this puts most sites with a low or negative ΔT value that are not multilayered in a separate class from multilayered sites with a high ΔT value. RCHs with ΔT $<$ 50% are located on significantly ($p < 0.001$) more level terrain than RCHs with ΔT $>$ 50%, with an average ($\pm$ 1 standard deviation) inclination of 2.8 $\pm$ 1.6° against 7.0 $\pm$ 3.0°, respectively. Therefore, we attribute sites with ΔT $<$ 50% to generally be on slopes $<$ 4° and sites with ΔT $>$ 50% to generally be on slopes $>$ 4°. For the sake of brevity, the first group will be labeled as class 1 RCHs and the latter as class 2 RCHs henceforth. The site diameters were measured slope parallel (*Dp*) and slope orthogonal (*Do*). Class 1 RCHs have an average *Dp* of 11.6 $\pm$ 1.3 m and a *Do* of 11.4 $\pm$ 1.6 m. Class 2 RCHs have an average *Dp* of 11.4 $\pm$ 1.6 m and a *Do* of 11.1 $\pm$ 1.4 m. Both classes of RCHs therefore showcase a slight ovality, with the longer axis in the slope parallel direction. However, the difference between *Dp* and *Do* is not statistically significant. Therefore, we subsequently assume a circular shape for RCHs on slopes, consisting of the averaged *Do* and *Dp* of each site.

A uniquely located site is RCH no. 38, which was surveyed in a bankside position next to a pond in the south of Hollenbeck. Due to groundwater influence we could only create a pit at position 2 in the middle of the platform on this site, therefore it could not be classified. Beside slope- and flat RCHs, we found one slope platform RCH surrounded by a ridge (no. 65) in the north of Hollenbeck as described by Hirsch et al. (2020) and Tolksdorf et al. (2020). RCH no. 35 could not be classified due to lacking a profile at the first position.

4.2. Slope correlation with ΔT and diameter

We used simple linear regression models to analyze the correlation of ΔT and diameter with slope inclination (Fig. 3). For class 1 RCHs there is a moderately weak positive and insignificant correlation of ΔT with the slope. ΔT ranges from −59% to 42%, which we regard as variation caused by the collier's efforts to create an even platform on generally flat positions with rough micro relief features (at the meter scale) that are not captured by our DEM-based slope measurement. For class 2 RCHs there is a moderate positive correlation of ΔT with slope, suggesting a general increase in Auh-layer thickness toward the downslope end of sites on steeper slopes. From around 5° to 7.5°, ΔT rises to a maximum of up to 300% and then varies between 100% and more than 500%. Class 2 RCH‘s diameter correlates moderately negative with slope, showing a general decrease of site diameter with increasing slope inclination from $>$ 15 m at 1° to around 8 m on 12°.

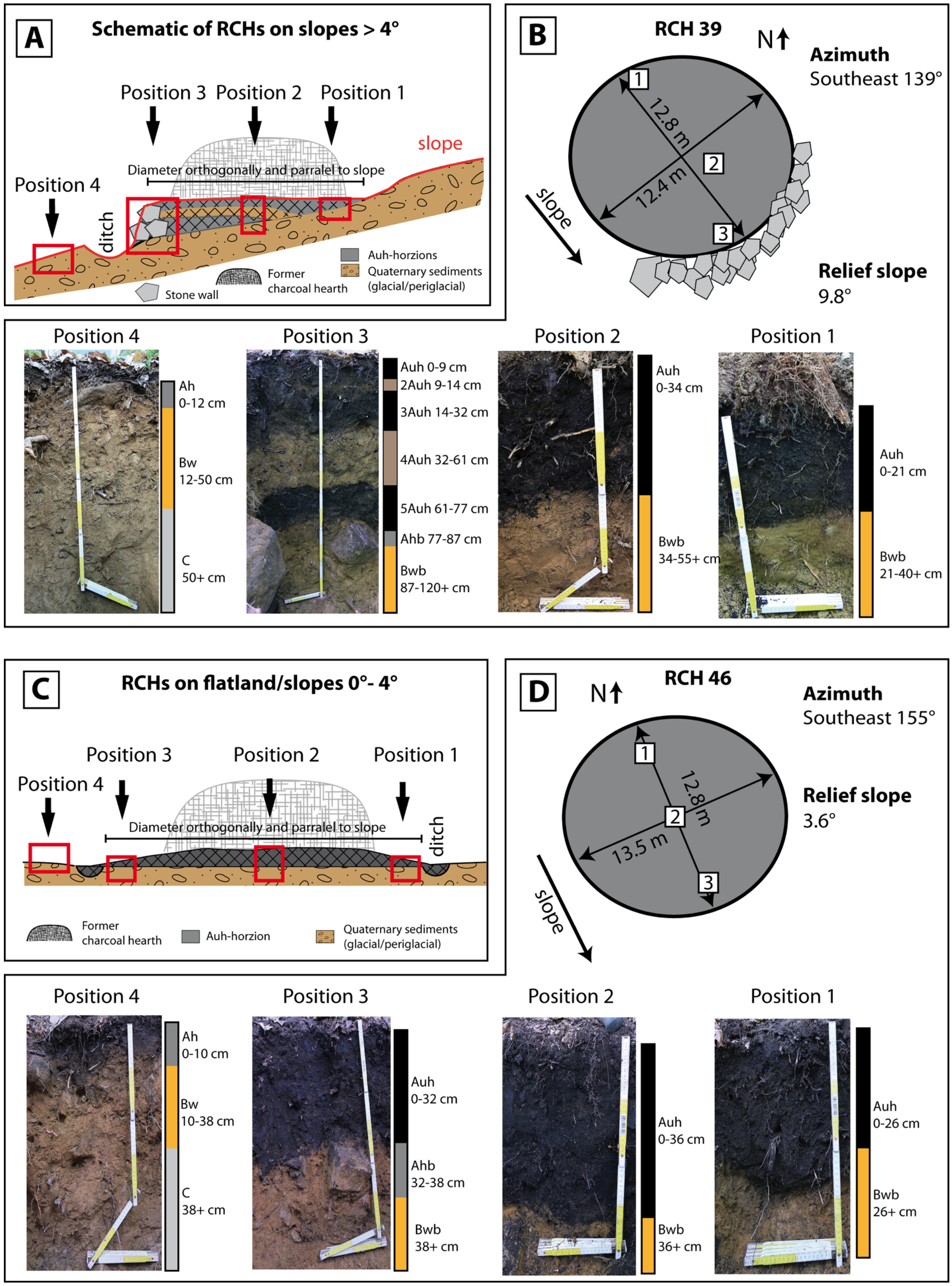

Fig. 2. Schematic of the two prevailing RCH types found in the study area, the position of sampling pits and the extent of the platforms diameter measurements: A) RCHs on slopes $> 4°$, with multiple technogenic layers; B) Example data and pit photos for RCH (no. 39), a high slope RCH; C) RCHs on slopes of $< 4°$ with a single technogenic layer; D) Example data and pit photos for RCH (no. 46), a low slope RCH.

4.3. *Site pedostratigraphy*

4.3.1. *Auh-layers*

The sites stratigraphy and their location alongside the transects is shown in Figs. 4 and 5. An overview of average thicknesses for all sites is given in Fig. 6 and Appendix B. Nearly every sites position has a primary Auh-layer with the exception of RCH no. 61, upon which no technogenic layer could be classified because of a distinct lighter color and comparably lower or lacking occurrence of charcoal pieces. RCH no. 38 and 35 are lacking two and one soil pits, respectively, hence the total number of Auh-layers per position in table 2 does not match the total number of RCH sites. The average first Auh-layer (Auh1) thickness increases from 20.9 ± 5.7 cm in position 1 to 23.6 ± 14.9 cm in position 3. The second Auh-layers (Auh2) average thickness is generally six to nine centimeter smaller then for the Auh1. The third Auh-layer (Auh3) is has an average thickness of 16.3 ± 9.7 cm. Neither Auh1,

Table 1
Wickwire RCH sites properties and the derived generalized classification of sites based on the difference (ΔT) in thickness of technogenic Auh layers between the up- (pos. 1) and downslope position (pos. 3) of a site (class 1: ΔT < 50%, class 2: ΔT > 50%). *Dp* and *Do* give the diameter of a site measured parallel and orthogonal to the slope.

RCH no.	Slope [°]	Dp [m]	Do [m]	Diameter Average [m]	Total Auh thickness pos. 1 [cm]	Total Auh thickness pos. 3 [cm]	ΔT [%]	RCH class
39	9.1	12.4	12.8	12.6	21	77	267	2
40	11.2	8.4	9.8	9.1	10	38	280	2
41	6.9	9.5	11.3	10.4	18	42	133	2
42	8.2	11.6	10.8	11.2	24	43	79	2
43	7.8	10.0	10.0	10.0	23	78	239	2
44	11.9	9.2	8.3	8.8	11	44	300	2
45	10.0	10.4	9.3	9.9	25	54	116	2
46	4.7	13.5	12.8	13.2	26	32	23	1
47	0.9	15.4	13.8	14.6	31	60	93	2
48	7.1	9.8	10.1	10.0	23	50	117	2
49	9.7	10.7	10.0	10.4	23	55	139	2
50	11.5	10.5	8.3	11.7	25	84	236	2
51	4.5	15.0	12.9	14.0	23	61	165	2
52	1.6	13.2	13.5	13.4	27	27	0	1
53	3.1	11.6	10.7	11.2	34	36	6	1
54	1.3	10.9	9.4	10.2	22	9	−59	1
55	4.0	12.8	11.3	12.1	24	55	129	2
56	6.9	11.3	11.3	11.3	10	62	520	2
57	6.6	12.6	12.1	12.4	20	70	250	2
58	11.3	11.5	11.0	11.3	18	50	178	2
59	6.6	9.5	13.3	11.4	18	60	233	2
60	5.3	9.9	9.7	9.8	15	63	320	2
61	3.5	8.4	8.4	8.4	5	5	0	1
62	10.4	10.6	10.4	10.5	18	60	233	2
63	2.1	12.1	11.1	11.6	24	33	37	1
64	6.4	11.8	13.8	12.8	27	30	11	1

Auh2, or Auh3 horizon thicknesses significantly correlate with slope inclination (data not shown).

4.3.2. Intermediate Auh-layers

The average thickness of the int Auh1 horizon increases from 7.6 ± 4.0 cm to 14.4 ± 7.3 cm. A second intermediate Auh-layer (int Auh2) is comparably rare. Its average thickness ranges from 8.5 ± 4.5 cm in position 2 to 24.0 ± 11.2 cm in position 3. Neither int Auh1 or int Auh2 horizon thicknesses correlate with the slope inclination (data not shown).

4.3.3. Forest soil horizons

We could identify buried Ah-horizons (Ahb) on 37 RCH sites, mostly on positions 2 and 3 (Appendix B), but only very seldom on both at the same site. Their distinguishing characteristics are the lack of macro and micro sized charcoal particles except for scattered pieces at the top of

Table 2
Hollenbeck RCH sites properties and the derived generalized classification of sites based on the difference (ΔT) in thickness of technogenic Auh layers between the up- (pos. 1) and downslope position (pos. 3) of a site (class 1: ΔT < 50%, class 2: ΔT > 50%). *Dp* and *Do* give the diameter of a site measured parallel and orthogonal to the slope.

RCH no.	Slope [°]	Dp [m]	Do [m]	Diameter Average [m]	Total Auh thickness pos. 1 [cm]	Total Auh thickness pos. 3 [cm]	ΔT [%]	RCH class
28	11.1	13.0	11.6	12.3	13	83	538	2
29	3.0	12.0	12.6	12.3	17	30	76	2
30	4.7	12.2	12.4	12.3	21	54	157	2
31	8.5	11.9	10.8	11.4	19	87	358	2
32	7.1	9.5	10.2	9.9	15	50	233	2
33	10.6	8.8	8.9	8.9	19	43	126	2
34	2.8	12.4	11.8	12.1	20	20	0	1
35	2.1	11.5	10.8	11.2	–	–	–	–
36	2.0	11.8	12.2	12.0	25	31	24	1
37	3.0	11.7	11.4	11.6	29	36	24	1
38	2.3	9.8	8.9	9.4	–	–	–	–
65	6.0	11.9	10.9	11.2	40	54	35	–
66	4.2	11.6	10.8	11.8	16	52	225	2
67	6.0	11.8	11.7	12.3	25	53	112	2
68	7.4	13.0	11.6	13.3	19	70	268	2
69	3.2	13.4	13.2	11.4	21	11	−48	1
70	1.5	11.6	11.2	11.1	24	44	83	2
71	5.6	11.2	11.0	12.2	16	45	181	2
72	4.6	11.5	12.8	12.6	30	54	80	2
73	0.6	12.3	12.8	11.9	35	23	−34	1
74	1.5	12.0	11.8	12.8	26	40	54	2
75	6.4	13.1	12.5	11.4	20	64	220	2
76	4.4	12.9	9.8	11.5	20	57	185	2
77	2.7	11.2	11.8	12.3	20	10	−50	1
78	0.3	11.9	12.6	9.4	26	16	−38	1
79	5.2	9.6	9.1	12.3	26	37	42	1

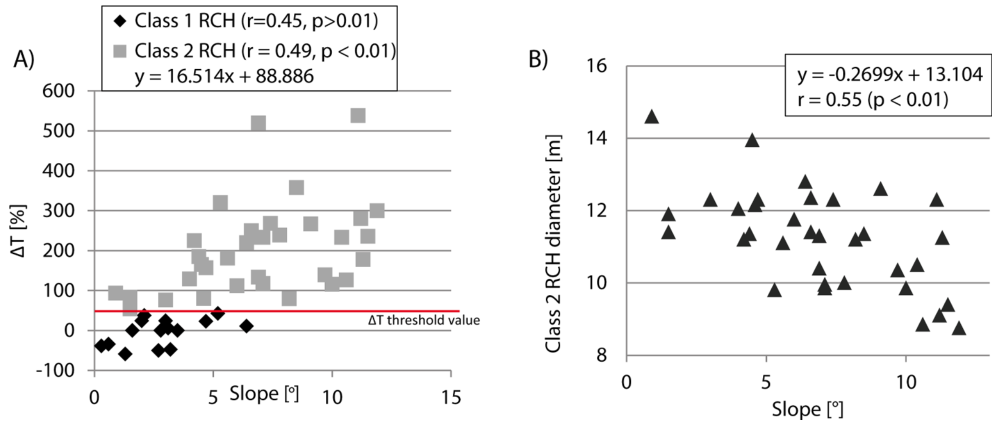

Fig. 3. A) Relationship between slope and downslope change in Auh-layer thickness (*ΔT*) for individual RCH sites; Right) Relationship between slope and class 2 RCH diameter.

the horizons, a less dark color then the Auh-layers and predominantly a very sharp upper boundary that is even, wavy or interlocked. The average Ahb thickness increases from 5.0 ± 2.2 cm in position 1 to 8.7 ± 5.1 cm in position 3. Although buried Bw-horizons are generally present at nearly every soil profile we sampled, it was only possible to measure their vertical extent down to the lower boundary at 18 sites. The average Bwb-horizon thickness is barely changing depending on the position on a site. At position 1 it measures 15.6 ± 4.6 cm, and at position 3 14.3 ± 2.7 cm. In the reference forest soil profiles, we measured the thickness of 26 Ah-horizons and 20 complete Bw-horizons. The Ah-horizons have an average thickness of 9.7 ± 4.6 cm. The average Bw-horizon is 29.1 ± 8.6 cm thick. 11 RCH sites show a slight redness of the top end of the Bwb-horizons mostly at position three, indication heat exposure (Hirsch et al., 2018b).

4.4. Variation of bulk density

We detected significant differences in the bulk density of soil horizons by intra- and inter site comparison (Appendix C). The lowest average bulk density is measured in the Auh1 at position 1 with 0.66 ± 0.10 g per cm^3, with an increase to 0.73 ± 0.10 g per cm^3 on position 3 (Fig. 7) (Appendix D). There is a significant difference between position 3 and positions 1 and 2. Furthermore, the bulk density for the Auh1 differs significantly from most other soil horizons, including Auh2. Auh2 and Auh3 combined have an average bulk density of around 0.82 g per cm^3. An insufficient sample amount in Auh2 at position 1 and in Auh3 overall prevent more detailed analysis. The bulk density for int Auh1 and int Auh2 horizon ranges between 0.86 ± 0.07 g per cm^3 and 0.92 ± 0.17 g per cm^3, with no significant difference between positions. Their bulk densities do not significantly differ in relation to other soil layers, except for Auh1 and the Bwb-horizon. The Ahb- and Bwb-horizons bulk density ranges between 0.92 ± 0.14 g per cm^3 and 1.12 ± 0.15 g per cm^3 for each position, with mostly no significant difference between them. The Ahb-horizon is ~ 0.3 g per cm^3 higher than the reference forest soil Ah-horizon. No significant difference in bulk density can be detected between the buried- and the reference forest soil Bw-horizon.

5. Synthesis and discussion

5.1. Generalizing pedostratigraphy and RCH diameter

The following section gives the outline for the model we propose to generalize the pedostratigraphy of the analyzed RCH sites. A previous study has used one type of RCH architecture and only one variable (diameter) to generalize RCH geometry throughout a landscape in the North German Lowland (Bonhage et al., 2020), which works well in flat terrain and with architectural homogeneous RCHs. We can show that in sloped terrain with multiple-layered RCH types, the slope inclination and the associated differences in pedostratigraphy must be regarded as well. The correlations we show of ΔT and diameter with the slope inclination are moderately good, with some degree of heterogeneity that can be attributed to a number of factors. The first is that the colliers could have deliberately used site locations on natural breaks in the slope, which would allow for RCHs with a lower ΔT on a steeper general slope. This factor is mentioned by Krebs et al. (2017) in their comprehensive research on site selection criteria for historical charcoal production. However, we could not find evidence for the intentional usage of slope breaks to build platforms. Due to the potential significant disturbance of buried soil horizons, as seen by the sporadic occurrence of buried A-horizons and the difference in thickness of Bw- and buried Bw-horizons, as well as the potential reworking of Auh-layers during multiple usages of the platforms, a trigonometrical check of the “true” slope the site was built upon, based on the depth of the technogenic Auh-horizons lower boundaries, is unreliable. Second, the Auh-layers with low bulk densities and increased SOM content are potentially prone to compaction due to mechanical compression and the decomposition of SOM. This might be especially the case for the Auh2 layers which are often characterized by slightly sloped horizon boundaries, contrary to historic documents that usually note the importance of a horizontal platform for the construction of the charcoal hearth (e.g., see Warren et al., 2012). Third, the position of the hearth on a platform could be variable. Former studies suggest that each consecutive usage of a site resulted in a larger platform and therefore the possibility to build a larger hearth (Hirsch et al., 2018a, Raab et al., 2017), however, it is possible that a smaller hearth was built on top of a larger platform, and the substrate of the platform was used to cover the wood heap. If in this scenario, for example, substrate was mainly taken from the upslope end of the platform, then ΔT would be skewed. Fourth, regarding the RCH diameters, heterogeneity can be caused by faulty or imprecise measurements in the field. Frequently it was not possible to identify clear boundaries of RCH platforms and the forest floor, in the slope parallel direction. Lastly, it must be considered that the colliers, although presumably using regionally appropriate construction techniques based on a principle of minimum energy expenditure, also varied the size of the constructed platforms depending on other factors, e.g., available workforce, intended reuse of sites, or wood availability. However, no further information is available on these aspects.

In light of these uncertainties, we propose a model based on RCH site slope inclination to account for the differences in the sites' pedostratigraphy and diameter. The resulting model is based on two assumptions: First, RCH sites in the study area can be classified into the RCH on slopes and the flatland RCH class that has been reported for this and study areas in Europe. Second, the fact that sites on slopes are

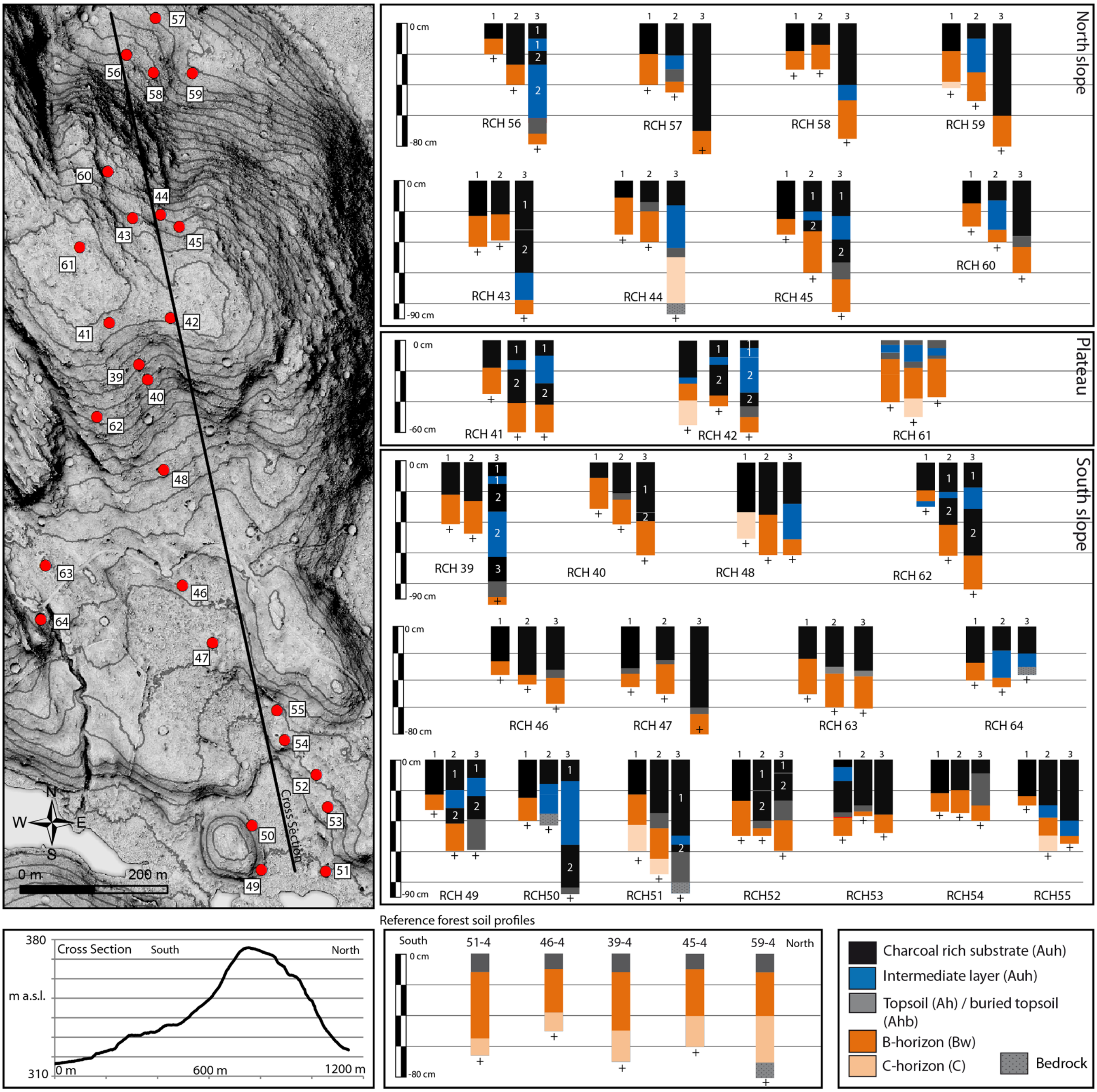

Fig. 4. Overview of Wickwire RCH site locations and summary of soil stratigraphy data. The map shows 1.5 m contour lines.

usually multilayered and sites on flatland are usually single layered and more or less constant in thickness holds true. We could show that both assumptions can be confirmed for our study area. The resulting two categories of idealized sites and their properties are listed in Table 3. The sites are categorized using a threshold value of 4° slope inclination based on results from Section 4.1. The 4° slope inclination break in the data is crucial for the differentiation of single- and multilayered sites when using the approach outlined in this study. The thickness of Auh-layers is not correlated with slope inclination, therefore an average horizon thickness can be assumed for all sites, which is potentially showcasing their artificial character and the lack of erosive slopewash. Colluvial deposits of substrate onto the RCH platform, whether caused by historic anthropogenic activity or natural processes, should potentially lead to a larger thickness of RCHs Auh-layers on steeper slopes. ΔT for class 2 RCHs correlates significantly with slope and can therefore be calculated for site specific inclinations. Under the assumption that the technogenic horizons at position 1 consist solely of a first Auh-layer, all the other layer thicknesses at position 2 and 3 can be calculated. For position 2, ΔT is thereby only half as thick as for position 3. The secondary Auh- and intermediate Auh-layer have an additional factor proportional to the summarized technogenic-layer thickness of position 2 and 3. At position 2 the summarized average thickness of the Auh1-, Auh2- and intermediate technogenic layers is 44.5 cm, whereof, based on their average thicknesses, 51% are made up of the Auh-1 layer, 32% of the Auh2-layer and 17% of the intermediate Auh-layer. For position 3 it's a total of 54.3 cm, whereof 41% are Auh1, 32% are Auh2 and 27% are intermediate Auh-layer substrate. The volume of the idealized soil-layer shapes can then be calculated as a cylinder for flat RCHs (Bonhage et al., 2020), and as the sum of three truncated cylinders for slope RCHs (Fig. 8). Stocks of elements can be calculated using the volume and average bulk densities for each soil-layer.

Bulk densities for Auh-layers in RCHs are typically lower than the

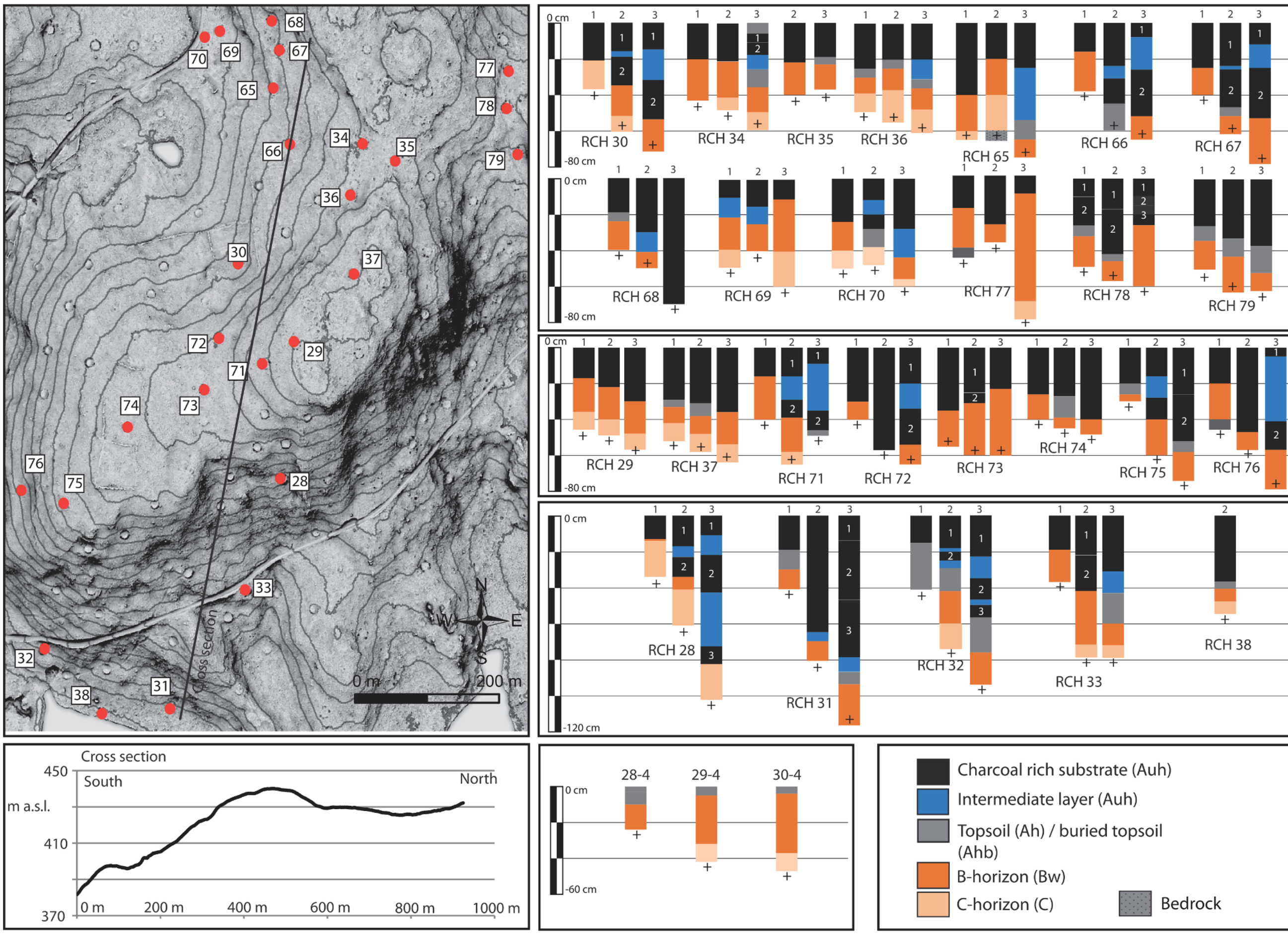

Fig. 5. Overview of Hollenbeck RCH site locations and summary of soil stratigraphy data. The map shows 1.5 m contour lines.

reference forest soils, as is the case for the first Auh-layer in this study. This is most likely linked to the high charcoal content as reported for this area (Hirsch et al., 2018a) and similar sites in Pennsylvania (Mikan and Abrams, 1995). The differences in Auh1 and Auh 2 and 3 bulk densities most likely originate from soil compaction affecting the latter two. Differences between position 1 and 3 may be caused by differences in SOM content on the sites. Future studies need to address the SOM distribution on RCH sites to analyze this aspect. Comparing our results to other studies reveals some similarities, although for a detailed analysis differences in soil texture, SOM content and compaction should be taken into account. For mountainous regions published bulk densities (g per cm^3) vary: 0.61–0.76 (Harz mountains, Germany, Borchard et al., 2014), 0.60 (Northern Italy, Criscuoli et al., 2017), 0.70 (Connecticut, USA, Hirsch et al., 2018a), 0.69 (Southern Belgium, Mastrolonardo et al., 2019) and 0.65–1.04 (Southeastern Pennsylvania, Mikan and Abrams, 1995). Higher bulk densities (g per cm^3) in general are reported for sites in less sloped, non-mountainous terrain: 0.7–0.9 (Central Italy, Mastrolonardo et al., 2018) and 0.94–1.28 (Northeast

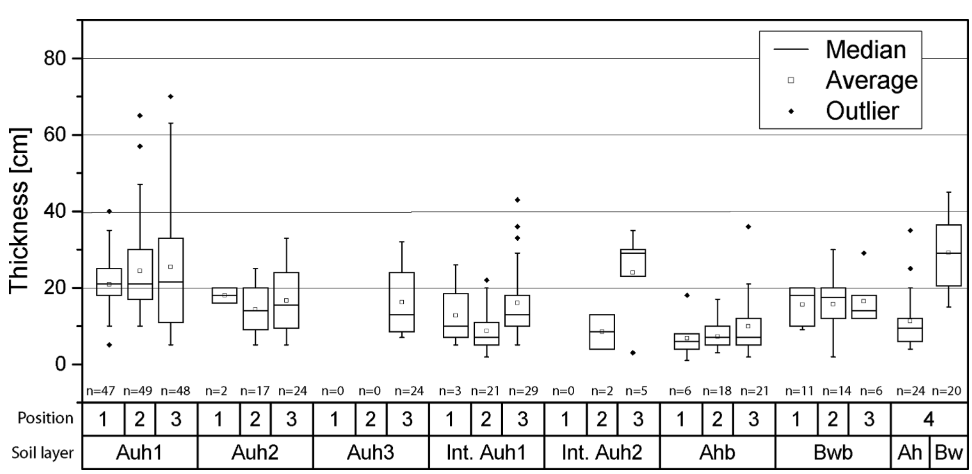

Fig. 6. Box and whisker plots comparing average soil horizon thickness and variation at the four positions of a RCH site (1: RCH upslope end; 2: center of the RCH; 3: RCH downslope end; 4: reference forest soil).

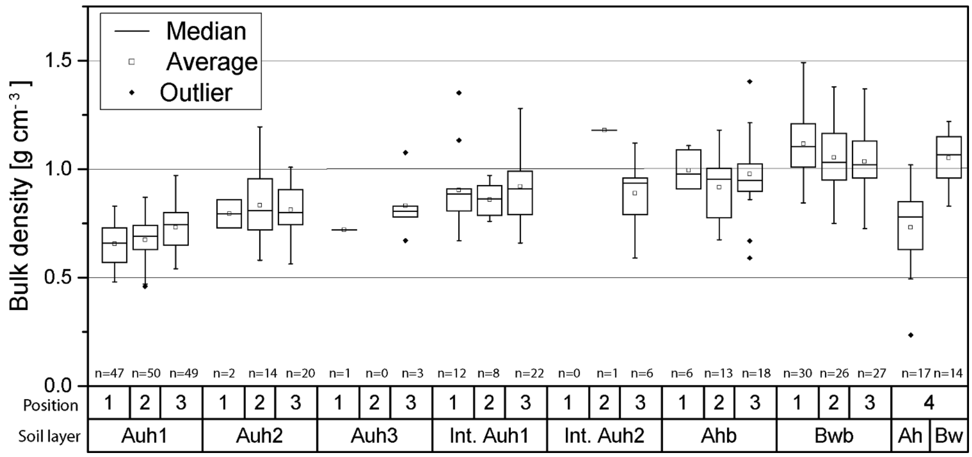

Fig. 7. Box and whisker plots comparing soil horizon bulk density and its variation at the four positions of a RCH site (1: RCH upslope end; 2: center of the RCH; 3: RCH downslope end; 4: reference forest soil).

Table 3
Parameters for the model of idealized RCH sites suitable for calculating geometry, pedostratigraphical thicknesses and stocks of elements.

	Ideal class 1 RCH	Ideal class 2 RCH		
ΔT [%] at position 3	0	ΔT = 16.514*slope[°] + 88.886		
Diameter	11.5 m	Diameter = −0.2699*slope[°] + 13.104		
Auh-layer Thickness	**Position 1,2,3**	**Position 1**	**Position 2**	**Position 3**
Auh1	22.6 cm	20.9 cm	22.9 cm	23.6 cm
intermediate Auh	–	–	(20.9*ΔT*0.01/2)*0.17	(20.9*ΔT*0.01)*0.27
Auh2	–	–	(20.9*ΔT*0.01/2)*0.32	(20.9*ΔT*0.01)*0.32
Bulk density g cm^{-3}				
Auh1	0.69 g cm^{-3}	0.69 g cm^{-3}	0.69 g cm^{-3}	0.69 g cm^{-3}
intermediate Auh	–	–	0.89 g cm^{-3}	0.89 g cm^{-3}
Auh2	–	–	0.82 g cm^{-3}	0.82 g cm^{-3}

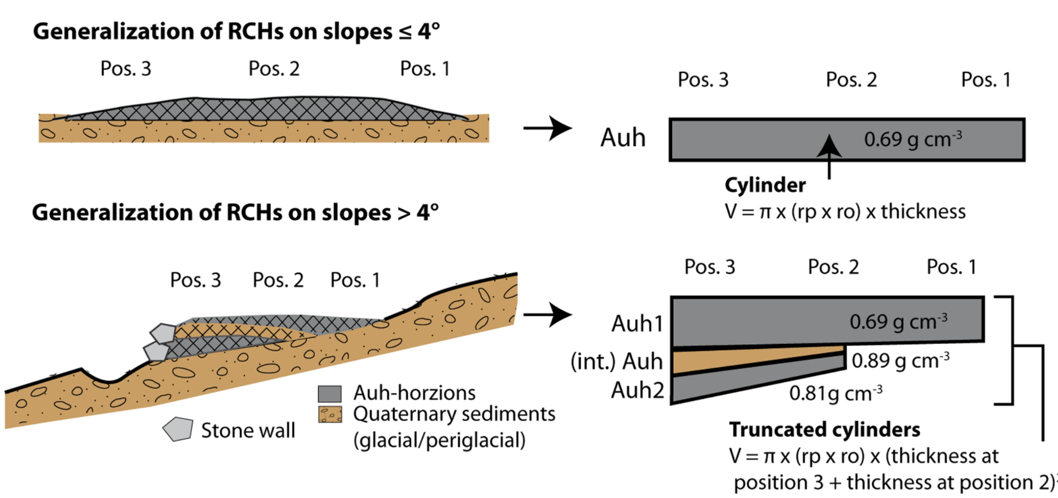

Fig. 8. Model for class 1 and 2 RCH architecture with generalized layers and average bulk densities for each soil layer.

Germany, Schneider et al., 2020a,b). To our best knowledge, this study is the first to report intra-site variations for multiple Auh and intermediate Auh-layers. Differences in bulk densities may impact physico-chemical soil properties important for forest ecological functions (e.g. Buras et al., 2020, Gießelmann et al., 2019, Carrari et al., 2018). Results from a year-long monitoring experiment show that the topmost 15 cm of technogenic RCH substrate has higher daily and seasonal temperature variations than adjacent forest soils, which is mainly due to the lower bulk density (Schneider et al., 2019). Increased preferential flow in technogenic RCH substrate under dry soil conditions can also lead to a high spatial and temporal variation of water contents. Because these effects are related to structural heterogeneity and hydrophobicity that results from high contents of charcoal and potentially by border effects from the boundary of technogenic- to forest soil substrate (Schneider et al., 2018a), they may be accentuated in multilayered sites.

5.2. Interregional comparison

A multilayered stratigraphy for RCHs on slopes is described here and in other sites studied in Connecticut, USA (Hirsch et al., 2018a,b, Raab et al., 2017). Stolz and Grunert (2010) describe up to four Auh-layers and corresponding intermediate layers at RCH sites that span a century of charcoal production in Southwest Germany. No information about the stratigraphy is given for RCH platforms in the foreland of the Taunus Mountain Range, Germany, however, sites are described as having a ridge at the downslope end that can be multilayered, representing multiple harvesting phases of a site (Stolz et al., 2012). Schneider et al. (2018b) document sites on slopes in Bavaria, Germany with a striking similarity to sites in this study, i.e. there are multiple Auh- and intermediate Auh-layers that increase in thickness towards the downslope end of the platform. Williams (2019) describes RCHs in Clarion County, Pennsylvania as being single layered and on mean slopes of 1.7° with diameters comparable to our study area, including the somewhat oval shape of the platforms. A LiDAR-based survey of RCH sites in the Blue Mountain Region, Pennsylvania describes that most sites there can be found on slopes of 8.5° − 11.3° Carter (2019), but unfortunately no further information about RCHs soil properties are known for that region. Otherwise, most studies of RCH sites have either no information on their stratigraphy, or describe them as single layered in case of flatland RCHs. The comprehensive comparison of Hirsch et al. (2020) documents several RCH architectural types that do not fundamentally vary for study sites in Central Europe and the US. This potentially indicates that our generalizations regarding the geometry of RCHs as a function of slope can be applied to other areas, since the dependency of layer thicknesses and slope should be the same. However, the lack of data regarding the detailed pedostratigraphy on different positions of RCH sites and its relation to slope for other regions limits the transferability for now, as it cannot be ruled out that multiple usages of RCHs site resulting in clearly discriminable Auh-layers is regionally specific. Furthermore, differences in geology or soils parent material can potentially limit the transferability of our results, e.g., as the presence of hard bedrock on the surface in the Ore Mountains (Saxony, Germany) required a different building technique for RCHs on slopes (Hirsch et al., 2020).

5.3. *Significance for geoarchaeology and beyond*

Overall, the study of RCHs in the geoarchaeological context is currently expanding in various disciplines. Advances regarding alteration of soil properties on RCHs and resulting effects on vegetation and fauna in relation to unaffected soils show the profound impact of this historical craft on present day forest ecosystems (e.g. Buras et al., 2020, Máliš et al., 2020) Furthermore, RCHs are potential sites of interest for the analysis of biochar application to soils and its degradation over time (e.g. Kerré et al., 2017, Borchard et al., 2014). Their charcoal content is a time capsule, potentially allowing the reconstruction of past forest compositions and historical wood exploitation. The geoarchaeological value of RCH sites originates not only from the possibility to more or less accurately date them by various techniques or by proxy of nearby historical industries, but also from the astonishing numbers in which they are mapped presently (e.g. Schneider et al., 2020a,b, Rutkiewicz et al., 2019). With this study, we show that it is possible to generalize RCH site shape with a model, allowing the transformation of site specific results onto a landscape scale. This is an important step towards understanding and quantifying the legacy effects of historical landuse on forest ecosystems. In this context, future studies should further assess the detailed stratigraphical properties of complete RCH platforms in different regions of the USA and Central Europe. Furthermore, detailed RCH site mappings on a landscape scale and spatial analysis regarding their topographical position are required to apply and test the presented generalizations.

6. Summary and conclusions

This study aims at producing a model to generalize the stratigraphical features of RCHs based on their position in the landscape. We show that RCH sites in western Connecticut exhibit two architectures with diameter and pedostratigraphies correlating to slope inclination. RCHs with an elevated circular construction type are characteristically located on flatter slopes ($< 4°$), while RCHs on levelled platforms are typically found on steeper slopes ($> 4°$). Sites on steeper slopes are usually multilayered and built up by multiple charcoal rich Auh-layers and intermediate Auh-layers consisting of reworked mineral substrate. Based on detailed study of 52 sites, we present a generalized model of RCH architecture that includes slope dependent variations of diameter, downslope Auh-layer thickness variation, individual Auh-layer thicknesses, and bulk density. The results show that an easy to implement model can be used to calculate soil volumes impacted by RCHs in landscapes affected by historical charcoal burning, and to assess effects on forest ecosystems such as additions to soil organic matter, changes in element stocks, and dynamics or modifications of soil biology or vegetation. Lack of data similar to that presented here regarding pedostratigraphy and soil physical properties limits further application into other regions where RCHs are common, such as Central Europe and mid-Atlantic USA. Future challenges include the assessment of the transferability of our generalizations into other regions, which depends on detailed field-based descriptions of the sites pedostratigraphy and its relation to the slope inclination. Furthermore, RCH site mappings on a landscape scale and knowledge about their soil properties are necessary to apply the presented generalizations.

Declaration of Competing Interest

The authors declare that they have no known competing financial interests or personal relationships that could have appeared to influence the work reported in this paper.

Acknowledgements

We want to thank Sally Donovan for supporting our field work. Furthermore, we like to thank three anonymous reviewers for comments that helped to significantly improve this manuscript. This research was supported by the German Research Foundation (DFG) under grant number RA 931/8-1. The funding source had no involvement in the study beside financial support. This work was also supported by National Science Foundation grant BCS-1654462 to W. Ouimet.

Appendix A. Physical and chemical soil properties for a representative RCH site (no. 39) and corresponding reference forest soil. Coordinates: 257377.089; 272519.568 (NAD_1983_2011_StatePlane_Connecticut_FIPS_0600_Ft_US).

RCH no. and pit position	Depth [cm]	Soil horizon	Bulk density [g cm^{-3}]	pH in $CaCl_2$	Munsell soil color code	Munsell soil color
39–4 reference forest soil	0–12	Ah	0.55	4.1	10YR 4/4	Dark yellowish brown
	12–50	Bw	–	4.5–4.7	10YR 6/8 – 2.5Y 7/6	Brownish yellow – yellow
	50–80	C	–	4.7	10YR 6/8 – 10 YR 5/4	Brownish yellow – yellowish brown
39–1	0–21	Auh	0.51	3.5–4.3	2.5Y 2.5/1 – 10YR 3/2	Black – very dark greyish brown
	21–40	2Bwb	–	4.5	10YR 7/4	Very pale brown

39–2	0–25	Auh	0.67	4.6–4.8	2.5Y2.5/1 – 10YR 2.5/1	Black – Black
	25–50 +	Bw2	–	4.8	10YR 7/4	Very pale brown
39–3	0–9	Auh	0.73	4.4	10YR 5/3	Brown
	9–14	2Auh (int)	0.94	4.8	2.5Y 6/4	Light yellowish brown
	14–32	3Auh	0.74	3.9–4.9	10YR 4/3 – 10YR 7/4	Very pale brown
	32–61	4Auh (int)	0.94	4.7–4.8	10YR 6/4 –10YR 3/2	Light yellowish brown - very dark greyish brown
	61–77	5 Auh	0.67	4.4–4.8	10YR 4/3 – 10YR 3/2	Dark greyish brown – brown
	77–87	fAh	1.14	4.8	2.5 Y 6/4 – 10YR 5/6	Light yellowish brown – yellowish brown
	87–120 +	Bw	0.96	4.2–4.4	10YR 6/8	Brownish yellow

Appendix B. Descriptive statistics of all measured soil horizons thickness for every position on the RCH sites and for reference forest soil profiles. Only Bwb- and Bw-horizons where the subsequent C-horizon was visible are included (SDW = Standard deviation, CV = Coefficient of variation).

Soil horizon	Position	N	Average thickness [cm]	SDW [cm]	CV
	1	47	20.9	5.7	0.3
Auh	2	49	22.9	8.1	0.4
	3	48	23.6	14.9	0.6
	1	2	18.0	–	–
Auh2	2	17	14.4	6.1	0.4
	3	24	17.4	8.5	0.5
	1	0	–	–	–
Auh3	2	0	–	–	–
	3	4	16.3	9.7	0.6
	1	3	8.3	2.5	0.3
Int Auh	2	21	7.6	4.0	0.5
	3	29	14.4	7.3	0.5
	1	0	–	–	–
Int Auh2	2	2	8.5	–	–
	3	5	24.0	11.2	0.5
	1	6	5.0	2.2	0.4
Ahb	2	18	6.7	2.6	0.4
	3	21	8.7	5.1	0.4
	1	11	15.6	4.6	0.3
Bwb	2	14	15.7	6.7	0.4
	3	6	14.3	2.7	0.2
Forest Ah	4	24	9.7	4.5	0.5
Forest Bw	4	20	29.1	8.6	0.3

Appendix C. Coefficient matrix of Mann-Whitney-*U* test results comparing bulk density for soil horizons (/ $p > 0.05$ (not significant), * $p \leq 0.05$, ** $p \leq 0.01$, *** $p \leq 0.001$).

Position		Auh1			Auh2		Ahb			Bwb			int Auh1			int Auh2	Ah	Bw
		1	2	3	2	3	1	2	3	1	2	3	1	2	3	3	4	4
Auh1	1	x	/	**	***	***	***	***	***	***	***	***	***	***	***	**	**	***
	2		x	**	***	**	***	***	***	***	***	***	***	***	***	**	*	***
	3			x	*	*	***	***	***	***	***	***	***	***	***	/	/	***
Auh2	2				x	/	*	/	*	***	***	***	/	/	/	/	/	***
	3					x	**	/	**	***	***	***	/	/	/	/	/	***
Ahb	1						x	/	/	/	/	/	*	*	/	/	***	/
	2							x	/	***	/	*	/	/	/	/	/	*
	3								x	**	/	/	/	*	/	/	***	/
Bwb	1									x	/	/	***	***	***	**	***	/
	2										x	/	**	***	**	*	***	/
	3											x	**	**	/	/	***	/
int Auh1	1												x	/	/	/	*	**
	2													x	/	/	/	**
	3														x	/	**	*
int Auh2	3															x	/	/
Ah																	x	***
Bw																		x

Appendix D. Descriptive statistics of soil horizons bulk densities for every position on the RCH sites and for reference forest soil profiles.

Soil horizon	Position	N	Average bulk density [g per cm^3]	SDW [g cm^{-3}]	CV
	1	47	0.66	0.10	15
Auh	2	50	0.67	0.09	13
	3	49	0.73	0.10	13
	1	2	0.80	–	–
Auh2	2	14	0.83	0.16	19
	3	20	0.81	0.12	14
	1	0	–	–	–
Auh3	2	0	–	–	–
	3	3	0.80	0.02	3
	1	12	0.90	0.17	19
Int Auh	2	8	0.86	0.07	9
	3	22	0.92	0.17	18
	1	0	–	–	–
Int Auh2	2	1	1.18	–	–
	3	6	0.89	0.16	18
	1	6	1.00	0.08	8
Ahb	2	13	0.92	0.14	15
	3	18	0.98	0.18	19
	1	30	1.09	0.13	12
Bwb	2	26	1.05	0.15	14
	3	27	1.04	0.14	13
Forest Ah	4	17	0.76	0.14	19
Forest Bw	4	14	1.05	0.12	11

Appendix E. Soil texture for RCH sites no. 28, 29, 30, 32, 33 (averaged per site) and their respective reference forest soil profiles (USDA texture triangle)

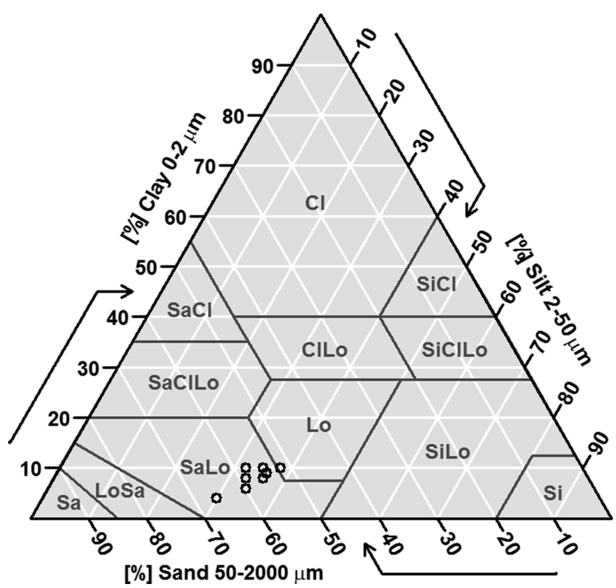

Appendix F. Coordinates for sampled RCH sites. (NAD_1983_2011_StatePlane_Connecticut_FIPS_0600_Ft_US)

RCH no.	X [m]	Y [m]
32	259,056	272,717
35	259,540	273,343
38	259,136	272,633
34	259,495	273,365
28	259,382	272,935
36	259,478	273,300
37	259,483	273,198
29	259,401	273,111
30	259,323	273,211
31	259,230	272,639
33	259,333	272,792
66	259,395	273,365

65	259,372	273,437
67	259,381	273,486
68	259,370	273,523
69	259,298	273,510
70	259,278	273,503
71	259,357	273,082
72	259,297	273,115
73	259,277	273,049
74	259,171	273,001
75	259,083	272,904
76	259,025	272,920
77	259,696	273,459
78	259,694	273,411
79	259,709	273,352
49	257,542	271,869
47	257,476	272,161
46	257,436	272,235
48	257,411	272,383
39	257,378	272,519
40	257,390	272,500
42	257,420	272,579
41	257,338	272,573
45	257,432	272,697
44	257,406	272,712
43	257,369	272,707
50	257,529	271,926
51	257,628	271,867
52	257,630	271,950
53	257,615	271,991
54	257,573	272,036
55	257,562	272,074
56	257,361	272,918
57	257,400	272,965
58	257,397	272,894
59	257,449	272,894
60	257,336	272,767
61	257,298	272,670
62	257,321	272,452
63	257,252	272,261
64	257,246	272,191

References

Bonhage, A., Hirsch. F., Schneider, A., Raab, A., Raab, T., 2020: Long term anthropogenic enrichment of soil organic matter stocks in forest soils - detecting a legacy of historical charcoal production. Forest Ecol. Manage. https://doi.org/10.1016/j.foreco.2019.117814.

Borchard, N., Ladd, B., Eschemann, S., Hegenberg, D., Maria Möseler, B.M., Amelung, W., 2014. Black carbon and soil properties at historical charcoal production sites in Germany. Geoderma 232–234, 236–242. https://doi.org/10.1016/j.geoderma.2014.05.007.

Buras, A., Hirsch, F., Schneider, A., Scharnweber, T., van der Maaten, E., Cruz-Garcîa, R., Raab, T., Wilmking, M. 2020: Reduced above-ground growth and wood density but increased wood chemical concentrations of Scots pine on relict charcoal hearths. Sci. Total Environ. (in print). https://doi.org/10.1016/ j.scitotenv.2020.137189.

Carrari, E., Ampoorter, E., Bussotti, F., Coppi, A., Nogales, A.G., Pollastrini, M., Verheyen, K., Selvi, F., 2018. Effects of charcoal hearth soil on forest regeneration: Evidence from a two-year experiment on tree seedlings. Forest Ecol. Manage. 427, 37–44. https://doi.org/10.1016/j.foreco.2018.05.038.

Carter, B.P., 2019. Identifying landscape modification using open data and tools: The charcoal hearths of the Blue Mountain, Pennsylvania. Hist. Arch. 53, 432–443. https://doi.org/10.1007/s41636-019-00171-1.

Criscuoli, I., Baronti, S., Alberti, G., Rumpel, C., Giordan, M., Camin, F., Ziller, L., Martinez, C., Pusceddu, E., Miglietta, F., 2017. Anthropogenic charcoal-rich soils of the XIX century reveal that biochar leads to enhanced fertility and fodder quality of alpine grasslands. Plant Soil 411, 499–516. https://doi.org/10.1007/s11104-016-3046-3.

Dupin, A., Sordoillet, D., Fréville, K., Girardclos, O., Gauthier, E., 2019. The taphonomic characterization of a charcoal production platform. Contribution of an innovative pair of methods: Raman analysis and micromorphology. J. Arch. Sci. 107, 87–99.

Dupin, A., Girardclos, O., Fruchart, C., Laplaige, C., Nuninger, L., Dufraisse, A., Gauthier, E., 2017. Anthracology of charcoal kilns in the forest of Chailluz (France) as a tool to understand Franche-Comte forestry from the mid-15th to the early 20th century AD. Quart. Int. 458, 200–213. https://doi.org/10.1016/j.quaint.2017.03.008.

Gießelmann, U.C., Borchard, N., Traunspurger, W., Witte, K., 2019. Long-term effects of charcoal on nematodes and other soil meso- and microfaunal groups at historical kiln-sites - a pilot study. Eur. J. Soil Biol. 93. https://doi.org/10.1016/j.ejsobi.2019.103095.

Hardy, B., Cornelis, J.-T., Houben, D., Leifeld, J., Lambert, R., Dufey, J.E., 2017. Evaluation of the long-term effect of biochar on properties of temperate agricultural soil at pre-industrial charcoal kiln sites in Wallonia, Belgium. Eur. J. Soil Sci. 68, 80–89. https://doi.org/10.1111/ejss.12395.

Hardy, B., Cornelis, J.-T., Houben, D., Lambert, R., Dufey, J.E., 2016. The effect of pre-industrial charcoal kilns on chemical properties of forest soil of Wallonia, Belgium. Eur. J. Soil Sci. 67, 206–216. https://doi.org/10.1111/ejss.12324.

Hirsch, F., Schneider, A., Bonhage, A., Raab, A., Drohan, P., Raab, T., 2020. An initiative for a morphologic-genetic catalog of relict charcoal hearths from Central Europe. Geoarch. (In press) https://doi.org/10.1002/gea.21799.

Hirsch, F., Raab, T., Ouimet, W., Dethier, D., Schneider, A., Raab, A., 2018a. Soils on historic charcoal hearths: Terminology and chemical properties. Soil Sci. Soc. Am. J. 81, 1427–1435. https://doi.org/10.2136/sssaj2017.02.0067.

Hirsch, F., Schneider, A., Bauriegel, A., Raab, A., Raab, T., 2018b: Formation, classification, and properties of soils at two relict charcoal hearth sites in Brandenburg, Germany. Front. Environ. Sci., 6. Article 94. doi: 10.3389/fenvs.2018.00094.

IUSS Working Group WRB, 2014. World Reference Base for Soil Resources 2014, update 2015. FAO, Rome, 181.

Johnson, K., Ouimet, W., Raslan, Z., 2015. Geospatial and LiDAR-based analysis of 18th to early 20th century timber harvesting and charcoal production in Southern New England. Geol. Soc. Am. Abstr. Programs 47, 65.

Johnson, M.K., Ouimet, W.B., 2014. Rediscovering the lost archaeological landscape of southern New England using airborne light detection and ranging LiDAR. J. Arch. Sci. 43, 9–20. https://doi.org/10.1016/j.jas.2013.12.004.

Kerré, B., Willaert, B., Smolders, E., 2017. Lower residue decomposition in historically charcoal-enriched soils is related to increased adsorption of organic matter. Soil Biol. Biochem. 104, 1–7. https://doi.org/10.1016/j.soilbio.2016.10.007.

Knapp, H., Nelle, O., Kirleis, W., 2015. Charcoal usage in medieval and modern times in the Harz Mountains Area, Central Germany: Wood selection and fast overexploitation of the woodlands. Quart. Int. 366, 51–69. https://doi.org/10.1016/j.quaint.2015.01.053.

Kokalj, Ž., Somrak, M., 2019. Why not a single image? Combining visualisations to facilitate fieldwork and on-screen mapping. Remote Sens. 11. https://doi.org/10.3390/rs11070747.

Krebs, P., Pezzatti, G.B., Stocker, M., Bürgi, M., Conedra, M., 2017. The selection of suitable sites for traditional charcoal production: ideas and practice in southern Switzerland. J. Hist. Geogr. 57 (1), 16. https://doi.org/10.1016/j.jhg.2017.04.002.

Ludemann, T., 2010. Past fuel exploitation and natural forest vegetation in the Black Forest, the Vosges and neighbouring regions in western Central Europe. Palaeogeogr. Palaeoclimatol. Palaeoecol. 291, 154–165. https://doi.org/10.1016/j.palaeo.2009.09.013.

Máliš, F., Bobek, P., Hédl, R., Chudomelová, M., Petřík, P., Ujházy, K., Ujházyová, M., Kopecký, M., 2020. Historical charcoal burning and coppicing suppressed beech and increased forest vegetation heterogeneity. J. Veg. Sci. https://doi.org/10.1111/jvs.12923. accepted – in press.

Mastrolonardo, G., Calderaro, C., Cocozza, C., Hardy, B., Dufey, J., Cornelis, J.-T., 2019: Long-term effect of charcoal accumulation in hearth soils on tree growth and nutrient cycling. Front. Environ. Sci. in press. doi.org/10.3389/fenvs.2019.00051.

Mastrolonardo, G., Francioso, O., Certini, G., 2018. Relic charcoal hearth soils: A neglected carbon reservoir. Case study at Marsiliana forest, Central Italy. Geoderma 315, 88–95. https://doi.org/10.1016/j.geoderma.2017.11.036.

Mikan, C.J., Abrams, M.D., 1995. Altered forest composition and forest development on historic charcoal hearths in southeastern Pennsylvania. Can. J. For. Res. 26, 1893–1898. https://doi.org/10.1139/x26-213.

Raab, T., Hirsch, F., Oumiet, W., Johnson, K.M., Dethier, D., Raab, A., 2017. Architecture of relict charcoal hearths in northwestern Connecticut, USA. Geoarch. 32, 502–510.

Rutkiewicz, P., Malik, I., Wistuba, M., Osika, A., 2019. High concentration of charcoal hearths remains as legacy of historical ferrous metallurgy in southern Poland. Quat. Int. 512, 133–143. https://doi.org/10.1016/j.quaint.2019.04.015.

Schneider, A., Bonhage, A., Raab, A., Hirsch, F., Raab, T., 2020a. Large-scale mapping of anthropogenic relief features - legacies of past forest use in two historical charcoal production areas in Germany. Geoarch. 1–17. https://doi.org/10.1002/gea.21782.

Schneider, A., Hirsch, T., Bonhage, A., Raab, A., Raab, T., 2020b. The soil moisture regime of charcoal-enriched land use legacy sites. Geoderma 366. https://doi.org/10.1016/j.geoderma.2020.114241.

Schneider, A., Hirsch, F., Raab, A., Raab, T., 2019. The temperature regime of a charcoal-enriched land use legacy soil. Soil Sci. Soc. Am. J. 83 (3), 565–574. https://doi.org/10.2136/sssaj2018.12.0483.

Schneider, A., Hirsch, F., Raab. A, Raab, T. 2018a: Dye tracer visualization of infiltration patterns in soils on relict charcoal hearths. Front. Environ. Sci. 6. Article 143. doi: 10.3389/fenvs.2018.00143.

Schneider, A., Hirsch, F., Raab, A., Raab, T. 2018b: Bodenkundlich-geomorphologische Untersuchung von Meilerplätzen um Weiherhammer. Beiträge zur Archäologie in der Oberpfalz und in Regensburg. 12. 433-448. ISSN 1617-4461.

Stolz, C., Böhnke, S., Grunert, J. 2012: Reconstructing 2500 years of land use history on the Kemel Heath Kemeler Heide, southern Rhenish Massif, Germany. 61. 169–183. doi:10.1016/j.quaint.2009.08.022.

Stolz, C., Grunert, J., 2010. Late Pleistocene and Holocene landscape history of the central Palatinate forest Pfälzerwald, south-western Germany. Quart. Int. 222, 129–142. https://doi.org/10.3285/eg.61.2.05.

Stone, J. R., Schafer, J. P., London, E. H., DiGiacomo-Cohen, M. L., Lewis, R. S., Thompson, W. B. 2005. Quaternary geologic map of Connecticut and Long Island Sound Basin. Reston, VA: U.S. Geological Survey.

Tarolli, P., Cao, W., Sofia, G., Evans, D., Ellis, E.C., 2019. From features to fingerprints: A general diagnostic framework for anthropogenic geomorphology. Prog. Phys. Geogr. 43, 95–128. https://doi.org/10.1177/0309133318825284.

Tolksdorf, J.F., Kaiser, K., Petr, L., Herbig, C., Kočár, P., Heinrich, S., Wilke, F.D.H., Theuerkauf, M., Fülling, A., Schubert, M., Schröder, F., Křivánek, R., Schulz, L., Bonhage, A., Hemker, C., 2020. Tracing past human impact in a mountain area: geoarchaeology of the medieval glass kiln site Ullersdorf, Erzgebirge Germany. Reg. Environ. 20, 71. https://doi.org/10.1007/s10113-020-01638-1.

Tolksdorf, J.F., Elburg, R., Schröder, F., Knapp, H., Herbig, C., Westphal, T., Schneider, B., Fülling, A., Hemker, C., 2015. Forest exploitation for charcoal production and timber since the 12th century in an intact medieval mining site in the Niederpöbel Valley (Erzgebirge, Eastern Germany). J. Arch. Sci.: Reports. 4, 487–500. https://doi.org/10.1016/j.jasrep.2015.10.018.

Verschoof-van der Vaart, W.B., Lambers, K., 2019. Learning to look at LiDAR: The use of R-CNN in the automated detections of archaeological objects on LiDAR data from the Netherlands. J. Comp. Appl. Arch. 2, 31–40. https://doi.org/10.5334/jcaa.32.

Warren, G., McDermott, C., O'Donnell, L., Sands, R., 2012. Recent excavations of charcoal production platforms in the Glendalough Valley, Co. Wicklow. J. Irish Arch. 21, 85–112. http://hdl.handle.net/10197/6578.

Williams, C.E. 2019: LiDAR prospection of relict charcoal hearths of the Shippenville Furnace region, Clarion County, Pennsylvania. Pennsylvania Archaeologist. 89.